Case Study

Hurricane Michael in the Area of Mexico Beach, Florida

Andrew Kennedy, M.ASCE[1]; Andrew Copp[2]; Matthew Florence[3]; Anderson Gradel[4]; Kurtis Gurley, M.ASCE[5]; Matt Janssen, S.M.ASCE[6]; James Kaihatu, A.M.ASCE[7]; Douglas Krafft[8]; Patrick Lynett, M.ASCE[9]; Margaret Owensby[10]; Jean-Paul Pinelli, M.ASCE[11]; David O. Prevatt, F.ASCE[12]; Spencer Rogers, M.ASCE[13]; David Roueche, A.M.ASCE[14]; and Zachariah Silver[15]

Abstract: Category 5 Hurricane Michael made landfall near Mexico Beach, Florida on October 9, 2018, with measured high water marks (HWMs) reaching 7.2 m NAVD88. The town itself received great damage, with many areas destroyed down to the foundations. In this study, we document the storm and its effects on the greater Mexico Beach area: hazard, structural damage, and their relationships. Wave and surge damage was nearly total for low-lying properties, but damage decreased greatly with increasing elevation. Major wave and surge damage was noted in Federal Emergency Management Agency (FEMA) X zones, which are out of the 100-year floodplain, and it is suggested that the 100-year storm is a deficient measure for categorizing flood risk. **DOI: 10.1061/(ASCE)WW.1943-5460.0000590**.

Introduction

Hurricane Michael made landfall 13 km (7 nautical miles) west of Mexico Beach, Florida, USA at 18:00 UTC (13:00 local) on October 9, 2018, as a Category 5 storm with maximum 1 min sustained winds of 140 knots (72 m/s), and a minimum central pressure of 91.9 kPa (Beven et al. 2019). Fig. 1(a) shows Michael's track and strength as it underwent rapid intensification before landfall, strengthening from Category 2 to 4 on the Saffir–Simpson scale within one 6 h period. Further intensification to Category 5 at landfall made Hurricane Michael the strongest storm ever recorded in the Florida Panhandle region. Before Michael, the strongest storm in the NOAA HURDAT2 database that made landfall within 65 nautical miles of Mexico Beach was Category 3 Hurricane Eloise (1975), which made landfall with 110 knot winds (57 m/s) 51 nautical miles (93 km) west of Mexico Beach near Miramar Beach, while unnamed 1851, 1877, and 1894 storms made landfall in the region with 100, 100, and 105 knot wind intensities respectively (51, 51, 54 m/s). Recently, Hurricane Kate (1985) was an 85 knot Category 2 (44 m/s) storm that made landfall almost directly over Mexico Beach (Landsea and Franklin 2013). Therefore, Michael was stronger than any that residents had experienced in their lifetimes, and was one of the strongest hurricanes by central pressure to make landfall in the continental US (Beven et al. 2019).

Michael generated catastrophic damage, with strong winds across the entire region and high storm surge and waves over the smaller area centered on Mexico Beach. Poststorm, a team of researchers traveled to the area to record perishable records of the waves, surge, and damage from October 13 to 15, and from November 1 to 8, 2018. This study is a partial record of observations, interpretations, conclusions, and recommendations made by the team. For this study, we define the area of Mexico Beach to include all coastlines from 85.434°W to 85.356°W [Fig. 1(b)]. This includes the town of Mexico Beach proper in Bay County, FL, and contiguous areas in Gulf County because development is essentially continuous over the region.

Wind, Waves, Surge, and Runup

The only in situ instrument measurement of Michael's waves and surge came from the United States Geological Survey (USGS)

[1]Professor, Dept. of Civil & Environmental Engineering, Univ. of Notre Dame, 156 Fitzpatrick Hall, Notre Dame, IN 46556 (corresponding author). ORCID: https://orcid.org/0000-0002-7254-1346. Email: andrew.kennedy@nd.edu

[2]Student, Dept. of Civil & Environmental Engineering, Univ. of Notre Dame, 156 Fitzpatrick Hall, Notre Dame, IN 46556. Email: acopp@nd.edu

[3]Student, Dept. of Civil and Environmental Engineering, Virginia Tech., 2000 Patton Hall, Blacksburg, VA 24061. Email: matthf6@vt.edu

[4]Student, Dept. of Civil & Environmental Engineering, Univ. of Notre Dame, 156 Fitzpatrick Hall, Notre Dame, IN 46556. Email: agradel@nd.edu

[5]Professor, Engineering School of Sustainable Infrastructure & Environment, Univ. of Florida, 365 Weil Hall, Gainesville, FL 32611. ORCID: https://orcid.org/0000-0002-5671-5123. Email: kgurl@ce.ufl.edu

[6]Student, Davidson Laboratory, Stevens Institute of Technology, Castle Point on Hudson, Hoboken, NJ 07030. Email: mjanssen@stevens.edu

[7]Professor, Dept. of Civil & Environmental Engineering, Texas A&M Univ., 3136 TAMU, College Station, Texas 77843-3136. Email: jkaihatu@civil.tamu.edu

Note. This manuscript was submitted on November 11, 2019; approved on March 2, 2020; published online on June 18, 2020. Discussion period open until November 18, 2020; separate discussions must be submitted for individual papers. This paper is part of the ***Journal of Waterway, Port, Coastal, and Ocean Engineering***, © ASCE, ISSN 0733-950X.

[8]Research Engineer, Engineer Research and Development Center, US Army Corps of Engineers, 3909 Halls Ferry Rd., Vicksburg, MS 39180. Email: douglas.r.krafft@usace.army.mil

[9]Professor, Dept. of Civil & Environmental Engineering, Univ. of Southern California, 3620 South Vermont Ave., Los Angeles, CA 90089. Email: plynett@usc.edu

[10]Research Engineer, Engineer Research and Development Center, US Army Corps of Engineers, 3909 Halls Ferry Rd, Vicksburg, MS 39180. Email: margaret.b.owensby@erdc.dren.mil

[11]Professor, Mechanical and Civil Engineering, Florida Tech., 150 W, Univ. Blvd, Melbourne, FL 32901. Email: pinelli@fit.edu

[12]Associate Professor, Engineering School of Sustainable Infrastructure & Environment, Univ. of Florida, 365 Weil Hall, Gainesville, FL 32611. Email: dprev@ce.ufl.edu

[13]Coastal Construction Specialist, North Carolina Sea Grant, UNC-W Center for Marine Science, 5600 Marvin Moss Lane, Wilmington, NC 28409. Email: rogerssp@uncw.edu

[14]Assistant Professor, Dept. of Civil Engineering, Auburn Univ., 1301 Shelby Center, Auburn, AL 36849. ORCID: https://orcid.org/0000-0002-4329-6759. Email: dbr0011@auburn.edu

[15]Postdoctoral Researcher, Dept. of Civil & Environmental Engineering, Univ. of Notre Dame, 156 Fitzpatrick Hall, Notre Dame, IN 46556. Email: zsilver.nd@gmail.com

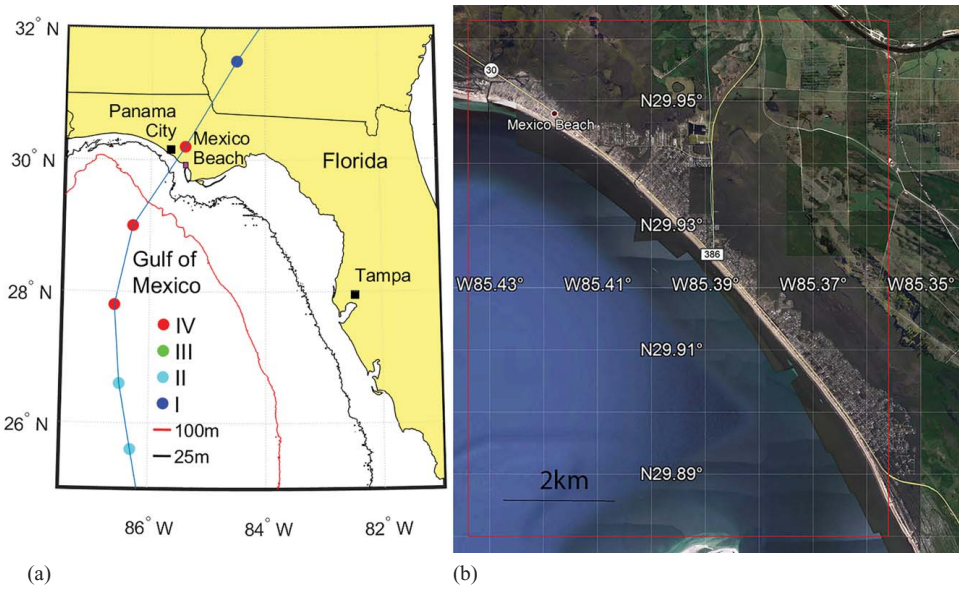

Fig. 1. (Color) Showing: (a) Hurricane Michael's track before and after landfall. Symbol colors denote Saffir–Simpson storm category, and the 25 and 100 m depth contours are as indicated. The small magenta inset immediately southwest of the Mexico Beach text indicates the study region; and (b) the spatial extent of the study location outlined in red, with NOAA poststorm airborne imagery overlying a satellite based background (base map imagery courtesy of NOAA).

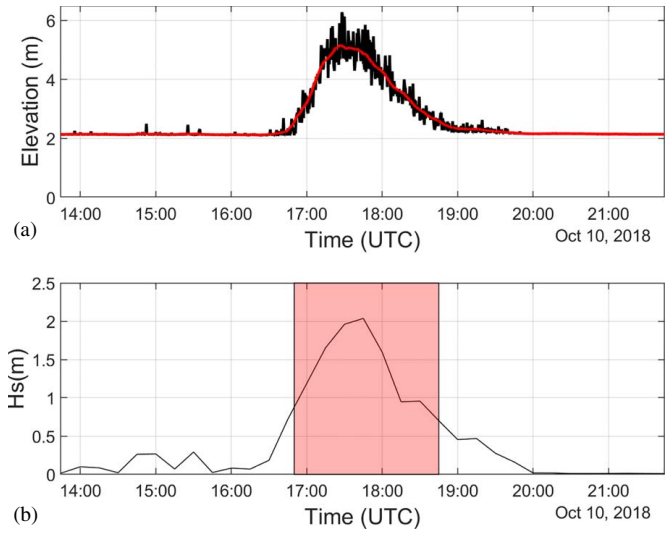

Fig. 2. (Color) Time series of water surface elevation (m) (NAVD88) from USGS gauge FLBAY03283 at the Mexico Beach Pier: (a) (—) unfiltered water level taken every 30 s; (—) moving 15 min average water level; and (b) significant wave height at pier. The shaded area represents the approximate time when the gauge did not go dry in wave troughs. Location is shown in Fig. 3.

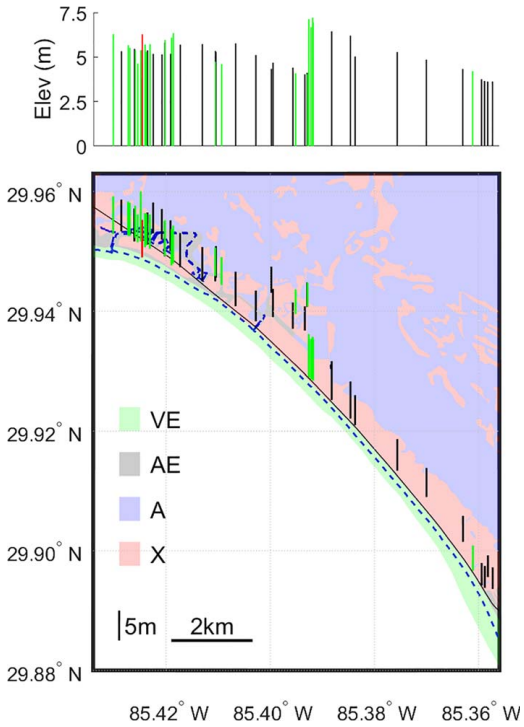

Fig. 3. (Color) HWMs in the vicinity of Mexico Beach: green represents measurements; black represents USGS; and red represents peak elevation from USGS sensor at pier. FEMA flood zones are as shown in the legend. Highway US98 is the solid black line close to the coast, and the NOAA shoreline is shown as a dashed line. Elevations are given in NAVD88 datum.

rapid gauge FLBAY03283, which was mounted on one of the pilings on the Mexico Beach Pier (Byrne 2019). The deck and almost all of the pilings seaward of the gauge were destroyed, but the gauge itself survived and provided good measurements. Fig. 2 shows a time series of the instantaneous water levels (computed using the hydrostatic assumption, and with atmospheric pressure, corrections using a nearby noninundated pressure gauge) measured every 30 s on October 10, and a 15 min average of these water levels which will be taken as the surge elevation. Fig. 3 shows the overall gauge location in Mexico Beach, and Fig. 4(a) shows a photograph of the gauge location poststorm.

Waves and surge began to rise consistently above the gauge elevation of 2.12 m North American Vertical Datum of 1988 (NAVD88), which is within 2 cm of the mean tide level in this area just before 17:00 UTC (12:00 local), reaching a surge peak of 5.16 m NAVD88, and a maximum instantaneous wave crest

J. Waterway, Port, Coastal, Ocean Eng., 2020, 146(5): 05020004

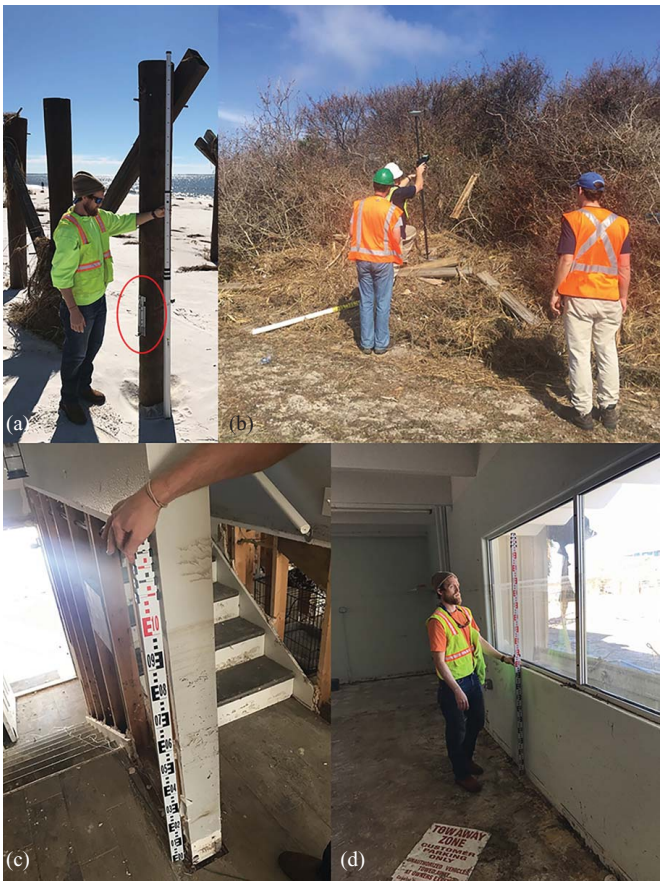

Fig. 4. (Color) Examples of water level measurements: (a) location of USGS water level gauge at the Mexico Beach Pier, with bracket location circled; (b) highest wave runup location; and (c and d) examples of interior watermarks. (Images by authors.)

elevation of 6.28 m (using the hydrostatic assumption) just before 17:30. These peaks were very short-lived, and by 19:00 only a few small wave crests were high enough to even reach the gauge. Realistically, most wave and surge damage probably occurred in the 1.5 h period between 17:00 and 18:30 UTC (12:00–13:30 local). This maximum wave crest of 6.28 m (20.6 ft) NAVD88 occurred in a National Flood Insurance Program (NFIP) 4.27 m (14 ft) VE zone (highest risk in the 100-year floodplain). No location in Mexico Beach (other than the pier in the ocean) had higher design elevations than this, while many inundated areas had much lower design elevations, and could be in the lower risk AE zones (moderate wave action in 100 year floodplain) or in Zone X (500 year floodplain) or Zone X (500-year floodplain) as shown in Fig. 3. Therefore, the conditions during Michael at Mexico Beach significantly exceeded design conditions for the 100-year flood plain.

Because water levels were only measured at 30 s intervals, no frequency information can be obtained about wave properties, but it is still possible to use the hydrostatic assumption to estimate time series of wave height at the pier. This is shown in Fig. 2(b), and was computed using $H_s = 4\sigma_W$ (Dean and Dalrymple 1991; Kennedy et al. 2011) where $\sigma_W =$ the standard deviation of water surface elevation over a 15 min period, after subtracting the filtered surge time series. Heights reached a maximum of just over $H_s \approx 2$ m very near to the time of peak surge when mean water depths were probably > 3 m above ground elevation (we do not know the ground elevation during the storm so it is not possible to say with certainty), therefore, these were highly nonlinear waves capable of causing great damage to structures and

Table 1. HWMs measured during this study

Latitude	Longitude	Elevation (NAVD88)	Description
29.952590	−85.426992	5.52	Mark inside building
29.952243	−85.425947	5.39	Mark inside building
29.951522	−85.425479	4.63	Mark in garage
29.952923	−85.430187	6.29	Eyewitness depth
29.956273	−85.424868	3.78	Wrack Line
29.945885	−85.410557	4.74	Mark inside building
29.939531	−85.395135	4.09	Mark in garage
29.940754	−85.392837	4.04	Mark in building
29.952648	−85.427314	5.67	Mark inside garage
29.951655	−85.424893	5.38	Mark inside house
29.951396	−85.424061	4.80	Mark inside house
29.951023	−85.423786	5.31	Mark inside house
29.950682	−85.424071	5.71	Mark inside house
29.950422	−85.423121	5.73	Mark inside house
29.947654	−85.418985	6.09	Scratches on building exterior
29.947964	−85.418643	6.35	Scratches on building exterior
29.949224	−85.420235	5.96	Impact marks on building exterior
29.896666	−85.361097	4.21	Mark inside house
29.944418	−85.409357	4.60	Debris
29.929031	−85.392606	6.35	Runup debris
29.929045	−85.392600	7.13	Runup debris
29.928708	−85.392183	6.69	Runup debris
29.928526	−85.391863	7.21	Runup debris
29.928436	−85.391760	6.95	Runup debris

Source: Data from Byrne (2019).

infrastructure. At times when the wave troughs could be lower than the gauge elevation, wave height values are lower bounds and Fig. 2(b) demarks these approximate times.

Although no other instrument records exist in the Mexico Beach area, both the present team and separately the USGS took numerous high water marks (HWMs). Table 1 lists the data taken during this study, while Open-file Report 2019-1059 references the USGS data as a freely available download (Byrne 2019). Both show a picture generally consistent with the water level gauge. Fig. 3 shows measured water levels from HWMs and the location of the USGS water level gauge. Wave runup elevations were taken near the tops of the main runup debris piles, and not the height of scattered debris which might have slightly higher elevations. Similarly, interior water marks were taken at the highest clear indication, and ambiguous waterlines were ignored. The water levels shown here are fairly conservative and, therefore, it remains quite possible that surge, runup, or both exceeded the values presented in Table 1. Fig. 4 shows examples of wave runup and HWMs, as well as the location of the USGS gauge at the Mexico Beach Pier.

The HWM elevations shown in Fig. 3 demonstrates both their changes in space and overall consistency. In the northwestern area of Mexico Beach, flow depths were large from the beach to US98, with many measurements of 5–6 m NAVD88. All of these HWMs were identified on surviving structures; no HWMs were found anywhere near the original shoreline, where waves were almost certainly larger. Moving southeast along the coastline, HWMs become significantly lower at around 85.4°W, at approximately 4–5 m NAVD88. This is probably because measurements here were quite far inland. However, HWM elevations increase strongly at approximately 85.393°W, where the beach is very narrow, and there are high ground elevations just across US98. Runup here exceeded 7 m in several locations as evidenced by undisturbed runup debris, with a maximum measured elevation of 7.2 m NAVD88 [Fig. 3(b)]. Moving further southeast along the coast, HWM elevations decreased almost monotonically, with all HWMs east of

85.36°W having elevations < 4 m NAVD88. This is both further from the storm center and the beginning of the area where sheltering from the St. Joseph Peninsula is important, therefore, the decrease is not unexpected. However, these maximum elevations of 4–7 m NAVD88 in the vicinity of Mexico Beach remain extreme and sufficient to deeply inundate much of the area.

Nearshore Erosion

Fig. 5 shows a small but typical section of the beach and the erosion that occurred during Michael. Poststorm (October–November 2018, US Army Corps of Engineers) and prestorm lidar (April–May 2017, Northwest Florida Water Management District) are used to create a difference map, with positive numbers showing the locations of erosion. Both datasets have standard errors listed as 10 cm, which are much lower than the differences seen pre to poststorm. Apart from Michael, there were no major storms in the region in between survey periods.

The major difference in prestorm and poststorm onshore data arises from the complete erosion of the coastal dune system, with up to several meters of elevation loss. Areas of deposition are seen landward in some locations and represent debris piles generated from more seaward houses and other moveable objects. Fig. 6 shows the two transects identified in Fig. 5 before and after the storm, which demonstrates the dune erosion. The dune crest elevations of approximately 4 m in transect 1 might also be compared with the peak surge value of 5.16 m NAVD88 and peak wave crest of 6.28 m NAVD88 measured at the nearby pier. These measured water levels greatly exceed the dune crest elevations, placing the system well into the inundation regime (Sallenger 2000) where sediment transport increases significantly and heavy dune erosion is expected. Once dune erosion was complete, large waves would have been able to penetrate inland with relatively little to impede them before encountering the many structures located close to the shoreline. Transect 2 provides a second example with no large fronting dunes, showing little overall erosion or accretion in the immediate beachfront area. However, both transects were chosen to intersect large debris piles, which were found in many inundated locations and will be assessed in more detail in the following sections. These debris piles showed large increases in elevation to the tops of debris, however, actual ground elevations underneath the debris had little to no erosion or accretion.

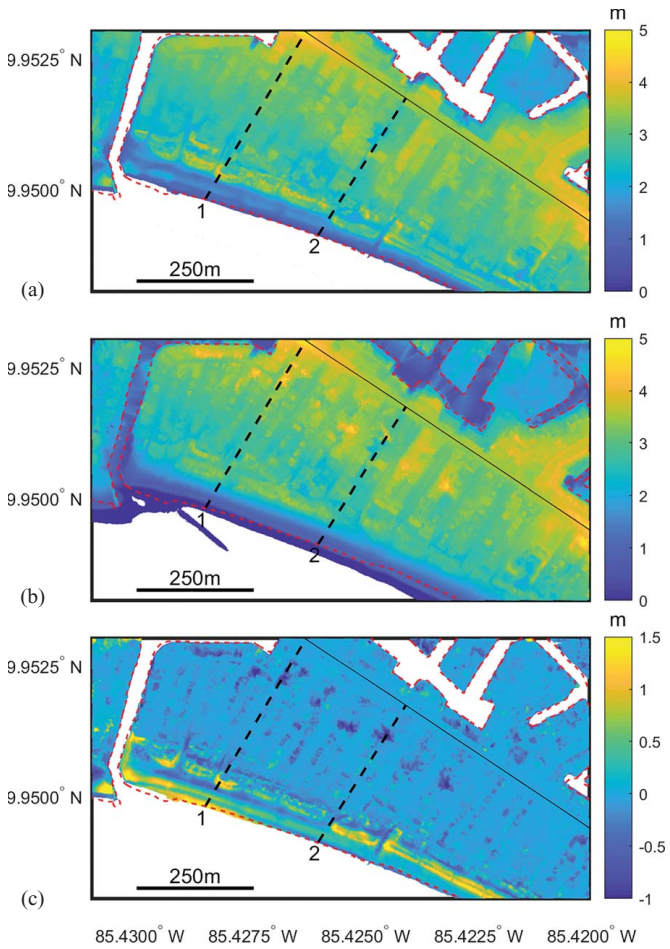

Fig. 5. (Color) Erosion example showing elevations in NAVD88 datum: (a) before; (b) after; and (c) difference. Erosion is shown as positive and deposition as negative. Elevations for transects 1 and 2 are shown in Fig. 6.

Infrastructure Damage

Infrastructure damage in the Mexico Beach region was severe and occurred from both wind and waves/surge. Critical facilities such as the Mexico Beach police and fire station were located well inland of US98 and did not experience significant damage from storm surge, but wind damage was observed. Fortunately, no hospitals or urgent care facilities were located in Mexico Beach, but the nearby larger regional center of Panama City contains many such facilities. Other critical infrastructures in Mexico Beach such as roads, telecommunication, and power infrastructure experienced various levels of impacts from both surge and wind, and there was no power, water, gas, or sewage available during the team's visits. Cellular service was restored rather quickly and was available throughout the town during reconnaissance.

Researchers noted partial washout of approximately 600 m of US98 in various locations between the western edge of Mexico Beach and HWY386 (a distance of approximately 5 km). A small vehicular bridge (span of approximately 15 m) across an inlet between 8th and 9th Streets collapsed, but a temporary bridge had

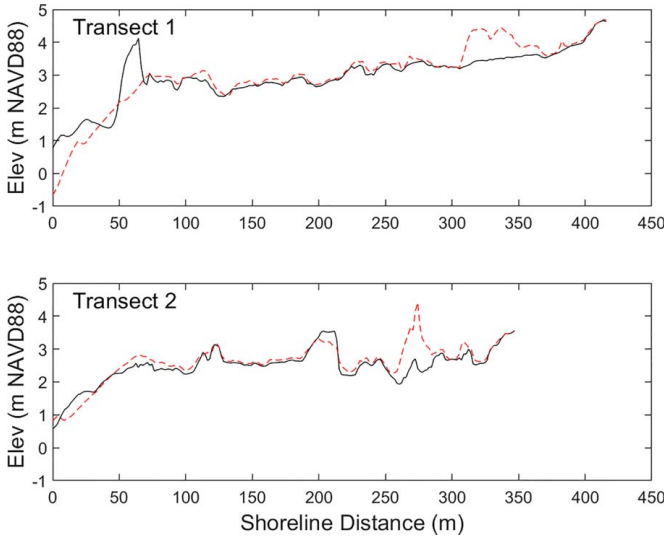

Fig. 6. (Color) Before storm (-) and poststorm (- -) bare earth elevation transects in NW Mexico Beach from the nominal shoreline to HYW98. Locations for Transects 1–2 are shown in Fig. 5.

already been installed by the time the damage assessments were conducted. Roueche et al. (2018) provide additional information on infrastructure impacted by Hurricane Michael.

Structural Damage

With very few exceptions, damage from Hurricane Michael's wind, waves, and surge ranged from severe to catastrophic in the area of Mexico Beach. Many ground elevations near the shoreline, in particular, in the western section of the study region, were 2.5–3 m NAVD88, meaning that inundation depths were great enough so that large damaging waves could reach structures once the dunes had eroded. This resulted in areas where entire blocks of buildings were destroyed down to their foundation slabs. More inland areas with smaller waves were not damaged as completely but still suffered significant inundation to walls, floors, and contents.

However, newer residential structures built according to the latest building codes, and far enough inland or at high enough elevations to escape waves and surge, in general, performed relatively well despite the extreme winds. Some newer and well elevated neighborhoods suffered, in general, little more than modest fenestration and roof cover damage. However, older structures were much more prone to severe wind damage, including significant roof cover and roof decking loss, which cascades into extreme water ingress and interior damage.

Near to the shoreline, the only structures that did not experience major damage were well built elevated structures, and even these generally lost utility connections and often staircases [e.g., Fig. 8(c)], and were prone to interior water damage from loss of soffits and damaged fenestration. Figs. 7 and 8 show examples of damage observed in the Mexico Beach area. Failure modes included the destruction of the entire structural frame (7a), structures detaching from foundations either at-grade (7b), or on top of piles (8a), loss of roof cover (7c), piled foundation loss of capacity or breakage (7d, 8a), wave damage to exposed structural components (8b), and erosional failures of foundations and associated components (8d). Observed structural failures are typical of a large wave and surge event (Robertson et al. 2007; Tajima et al. 2014; Tomiczek et al. 2014; Hatzikyriakou et al. 2016) where inundation depths are large and waves can generate destructive loading on exposed structures.

To evaluate surge and wave induced damage patterns, it is helpful to examine aggregate damage results over the Mexico Beach area. Many different researchers in the field gave preliminary structural assessments. These included photographs, elevations, descriptions, and damage ratings by component and overall. Separate postreconnaissance researchers used the field photographs to reassess the assessments for consistency and to translate damage ratings to those of Tomiczek et al. (2017). For a given property, the individual performance of various structural components was evaluated to produce an overall rating between DS0 (no observed damage) and DS6 (structure removed from the foundation) using the directions in Table 2. Roof damage was neglected in this scheme because roof damage to standing structures was almost certainly caused by extreme wind.

Elevations of lowest horizontal structural members (LHMs) concerning wave crest elevations are extremely important to structural survival. These elevations were obtained using lidar based bare earth digital elevation models (DEMs) taken post Michael to give ground elevations in NAVD88 datum, which were added to LHM heights above grade, either measured in situ with rods or more approximately using Google Street View based LHM height estimates (e.g., Tomiczek et al. 2017). Final LHMs reported here are in NAVD88 datum. The year of construction was taken from online

Fig. 7. (Color) Examples of structural damage: (a) destruction of at-grade house (DS6); (b) at-grade house detached from its foundations by waves and surge (DS6); (c) damaged at-grade house (note sheets of asphalt detached from road) (DS3); and (d) failure of prestressed concrete piling (DS6). (Images by authors.)

J. Waterway, Port, Coastal, Ocean Eng., 2020, 146(5): 05020004

Fig. 8. (Color) Examples of structural damage: (a) complete failure of pile elevated house (DS6); (b) severe damage to beachfront pile elevated row houses (DS5); (c) minor damage to Sand Palace (DS3); and (d) scour and partial failure of concrete floor pad underneath pile elevated house (DS5). (Images by authors.)

county resources and offline property databases. Because the region had significant changes in inundation moving NW–SE, the overall coastline was divided into subareas as shown in Fig. 9: either four (a–d) or two (N–S) depending on the properties considered.

Seaward of US98, there were four major types of construction: (1) older single family, at-grade homes made of concrete masonry units or brick; (2) connected townhouse type structures, typically timber frame; (3) pile elevated wood framed single family homes and small businesses; and (4) pile elevated multifamily residential or commercial construction. As expected, at-grade construction performed very poorly near the shore, with the frequency of survival increased with increasing distance inland. A poststorm assessment was made for all structures and the remains of structures that could be identified south of US98 between the western edge of Mexico Beach and the small bridge just west of 8th street (85.4028° W), and a less complete assessment further east to approximately 85.35°W. In many cases, multifamily units were treated as one structure when performance was similar, but individual units were also separated when differences were noted.

Fig. 10 shows the overall surge and wave induced damage ratings for all structures surveyed by the team in the Mexico Beach area, divided into the four subregions shown in Fig. 9. It is clear that in area (a) (furthest NW), large areas near the shoreline suffered complete damage, while the furthest SE section (d) showed areas near the shoreline with damage, but not anywhere near the extent of (a), with (b–c) demonstrating intermediate levels of damage.

The damage state was found to be a strong function of structural elevation as shown in Fig. 11, in particular, close to the shoreline. This is not at all surprising, because structures at higher elevations may encounter waves and surge for a shorter length of time, or not at all if they are sufficiently elevated. Structures built at-grade were almost universally destroyed in the most severe conditions near the shoreline (DS6) and were largely older single family houses. Structures at higher elevations demonstrated much higher survivability, although many of them still sustained significant damage. Further inland, structures experienced an increased chance of survival both from the higher ground elevations and the dissipating wave heights, but damage still tended to be severe. Very few structures surveyed had damage states less than DS2. Subregions (c–d) (SE Mexico Beach) showed lower damage states inland of US98, which will be explored in more detail in the following sections.

There were examples of good design and practice, the most impressive structural survival was the famous Sand Palace house built in 2018 and shown in Fig. 8(c). Although it is in the first row of houses near the region of worst surge and damage, the Sand Palace only had damage to: (1) utilities and local HVAC destroyed; (2) exterior staircase and lower story breakaway walls and interior destroyed; (3) a cracked window on the top floor; (4) one electrical outlet on the top floor ceiling popped out of its socket due to the pressure difference between the house interior and attic; (5) damage to parking slab and pavers; (6) minor water intrusion; and (7) one porch ceiling damaged. No roof damage was recorded. By the time of the team's visit, the owners had installed solar panels and batteries to provide electricity and except for town utilities were fully functional. The Sand Palace was in DFIRM Zone AE, elevation 12 ft (3.66 m) NAVD88, while the measured elevation of the LHM was 6.3 m (20.7 ft) NAVD88. This elevation almost exactly matched the largest measured wave elevation of 6.28 m NAVD88 measured at the nearby pier. Because the pier was slightly seaward of the Sand Palace, wave crest elevations at the house would likely have been slightly lower. Therefore, the largest wave crests during the storm came close to or barely touched, the LHM, and wave loads were certainly much lower than those experienced by houses at a lower elevation. As reported, the Sand Palace costs approximately 15%–20% additional per square foot when compared with standard construction practices (Dal Pino 2019). After Michael, and compared with its neighbors, this additional cost appears very well spent. This study also demonstrates that community

Table 2. Damage state component classification methodology

Component	0	1	2	3	4	5	6
Roof	• No visible damage	• Very few shingles missing (<15% of roof area) • Damage to gutters	• Significant amount of shingles missing 15%–50% of roof area) • Interior of roof is NOT exposed	• Many shingles missing >50% of roof area) • Damage to roof frame	• Holes in roof due to debris or wind-sheathing is exposed but not house interior	• Large parts of roof are missing or collapsed; house is still intact	—
Walls	• No visible damage	• Minor cladding removal (<10% of 1 wall) • Small scratches causing aesthetic damage	• Cladding has been removed from >10% of 1 wall or from multiple walls • Interior sheathing exposed on <10% of house	• Cladding has been removed from >25% of walls • >10% of sheathing is exposed but insulation and house interiors are not	• Minor structural wall damage, including debris caused holes or repairable damage	• Walls have collapsed, bent or are out of plumb, structural damage • Large holes in walls • Major structural damage	—
Foundation	• No visible damage	• Scour <0.5 feet deep around foundation • Water marks around foundation • Structurally sound	• Scour 0.5–1″ deep • Structurally sound foundation • Evidence of weathering on piles	• Scour is between 1′ and 2′ • Structurally Sound Foundation • Minor damage to piles	• One pile out of plumb, or damaged • Scour >2′ deep • Minor damage to foundation	• Major but reparable foundation damage • House has differentially settled • >1 pile is damaged	• House is missing • Irreparable foundation damage
Attachments and detached structures: stairways, breakaway walls, air conditioning, sheds, etc.	• No visible damage	• <2 Exterior AC, pipes, etc., have been damaged or removed • Damage to stair, porches, detached garage, or walkways, most structures remain in tact	• 2 or more exterior amenities (stairways, electrical wiring, etc.) are gone or destroyed • Severe damage to decks, detached garages, etc.	• Detached structures destroyed/missing	—	—	—
Openings: windows, doors, attached garages	• No visible damage	• 1 window or door is broken (glass only) • Screens may be damaged or missing	• >1 window is broken but damage is all on lower story of 2+ story houses • <4 total openings are damaged • Damage to frames of doors and windows	• 4 or more windows and doors are broken • 1 or more doors was removed • Damage to windows /doors on upper levels • Attached garage door damaged or gone (bent or otherwise broken)	—	—	—

Table 2. (*Continued.*)

Component	0	1	2	3	4	5	6
Interior	• No visible damage	• Minor flood damage • Minimal/no evidence of rain intrusion- minor water damage in corners or around windows only • Minor water damage to interior furnishings	• Evidence of flooding • Water marks (0–1′) above floor • Evidence of rain intrusion- dampness/ water damage on <10% of wall area (one wall) • Wet spots observed on <10% of ceiling, no sagging • Water damage to interior furnishings	• Significant flooding • Water marks (1′–2′) • Ceiling damage from rain- wet spots, evidence of dripping 10%–50% of ceiling area • Dampness on 10%–50% of wall areas • Mold	• Water marks (2′–4′) • Ceiling water damage affecting stability- wet spots over 50%,evidence of dripping and sagging • Dampness on >50% of wall areas • Evidence of dripping or cracks on walls	• Water marks 4′ or higher • Ceiling damage from rain- wet spots and sagging • Structural Damage to interior walls (not fixable)	—

Source: Reprinted from Tomiczek et al. (2017), ©ASCE.

Fig. 9. (Color) Locations of subregions a–d, and N–S used in Figs. 10, 13, 15, and 16. The red asterisk shows the eastern end of the region where all structures seaward of US98 were evaluated for damage.

resilience to natural hazards is only effective when the plurality of infrastructure is similarly mitigated. Therefore, the Sand Palace is a win for the owners, but the community they returned to requires long term recovery efforts.

Damage by FEMA DFIRM Zone

Consideration of damage state compared with the structural elevation shows interesting patterns. General risk categories may be given by the Federal Emergency Management Agency (FEMA) definitions for their Digital Flood Insurance Rate Maps Zones VE and AE are designated Special Flood Hazard Areas, and flood insurance is "mandatory with mortgages from federally regulated or insured lenders." VE zones are areas "defined by the 1% annual chance (base) flood limits (also known as the 100-year flood) and wave effects 3 feet or greater." (https://www.fema.gov/media-library-data/20130726-1541-20490-5411/frm_p1zones.pdf). These areas have the greatest risk from 1 in 100-year surge and waves. One step down from this is the AE zone. These are defined with Base Flood Elevations (BFEs) "that reflect the combined influence of (100 years) still water flood elevations and wave effects less than 3 feet." During Michael, it is clear that surge and waves greatly exceeded the 100-year inundation, and for this reason, we will combine VE and AE zones since both almost certainly experienced large destructive waves.

The X zone in the Mexico Beach area is, for this study, the region not in the 100-year flood plain. In practice, many homeowners take the X zone as a region with no real hazard and do not obtain flood insurance. During Michael, the hazard was severe, and Fig. 10 shows that very many structures in the X zone were destroyed. Most of these structures were quite old and at low elevations, particularly in NW Mexico Beach. As shown in Fig. 10, entire sections of X zones were wiped clean to their foundations. Further south in subareas (c) and (d), there was a much greater frequency of survival and lower damage in X zones.

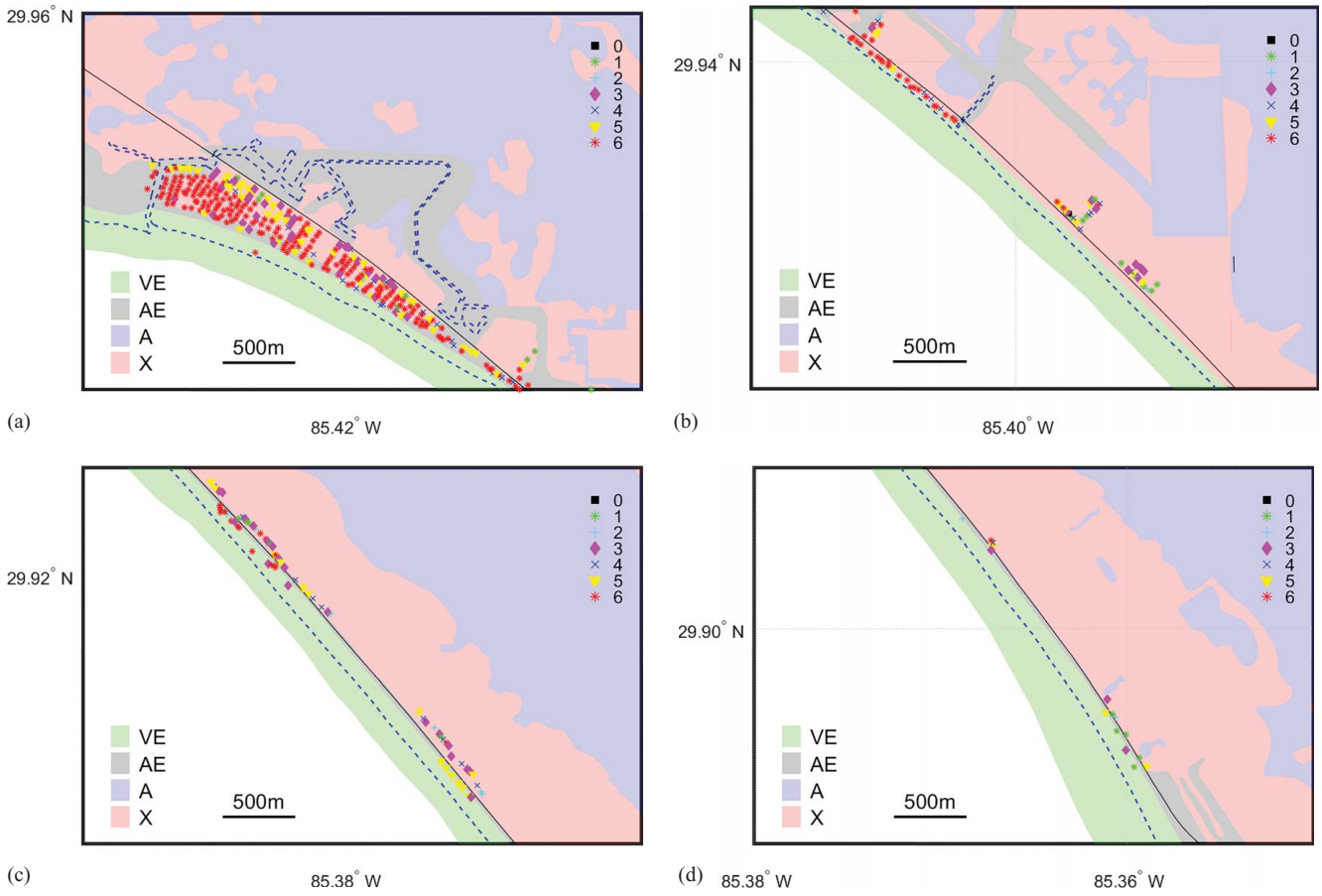

Fig. 10. (Color) Surge and wave induced structural damage states as in Tomiczek et al. (2017). Black square = DS0; green diamond = DS1; cyan + = DS2; magenta diamond = DS3; blue x = DS4; yellow triangle = DS5; red * = DS6: (a) subregion a; (b) subregion b; (c) subregion c; and (d) subregion d. FEMA DFIRM flood zones are as labeled.

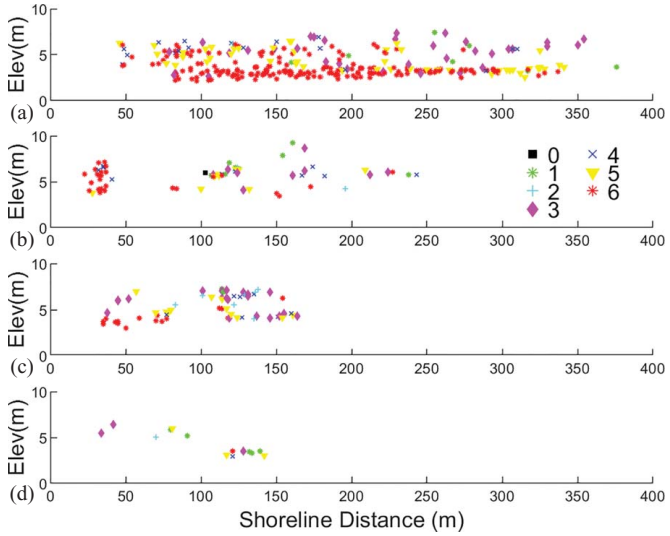

Fig. 11. (Color) Damage state versus elevation of LHMs in m NAVD88, and distance from shoreline in the subregions (a–d) as shown in Fig. 9.

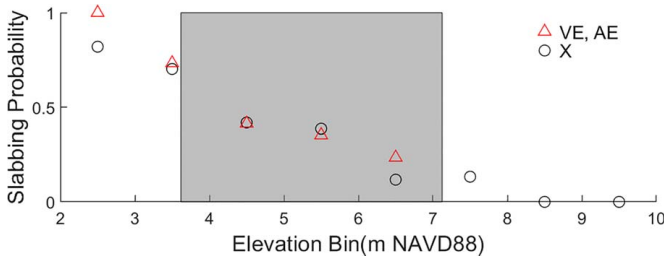

Fig. 12. (Color) Slabbing probabilities as a function of elevation over the Mexico Beach region for combined VE and AE zones (triangle); X zone (circle). The shaded region shows the range of observed HWMs.

The immediate survival or destruction of a structure is an important safety consideration. In this study, destruction is defined by damage category DS6, where the structure is slabbed; that is to say, it is completely removed from its foundations. Fig. 12 shows the probability of slabbing during Michael for aggregated VE–AE zones and X zones. Unsurprisingly, the probability of survival increases strongly with increasing building elevation. Somewhat surprisingly, the probabilities for VE–AE and X zones are almost identical, indicating that structural elevation was the overwhelming factor for survival. Because there was a range of inundation over the Mexico Beach region, this is reflected in the slabbing probabilities. Because Michael so greatly exceeded the 100-year event, the near coast DFIRM zones behaved like one. We note that this study looks almost exclusively at structures in the first few hundred meters from the shore, and slabbing behavior would certainly be different further inland.

Although all DFIRM zones showed similar slabbing probabilities when aggregated over the entire dataset, there were noticeable north–south differences. As shown in Fig. 3, inundation decreased notably at the far southeastern end of Mexico Beach. There was a corresponding decrease in the frequency of slabbing, as shown in

J. Waterway, Port, Coastal, Ocean Eng., 2020, 146(5): 05020004

Fig. 13. Structures in the southern area had a survival probability roughly equivalent to a 1–2 m higher structure in the northern portion of Mexico Beach. In this case, elevation relative to inundation appears to be the defining factor. The one exception is for elevations of 2–3 m in South Mexico Beach, with only 1 structure measured in this bin and correspondingly low confidence in the 0 probability of slabbing. This structure was landward of US98 and suffered major damage but remained standing.

Debris Generation and Transport

The destruction of structures and infrastructure generated large amounts of debris, much of which was transported inland. Fig. 14 shows typical examples of debris and debris piles. These could be quite large at times for both plan area and height above ground, as shown in the transects in Fig. 6. On a large scale, this debris was composed of entire structures detached from their foundations, cars, boats, and other transportable large objects. Debris at the smaller scales included household goods and fractured components of structures and infrastructure. The sheer quantity of debris remaining within the town was large both because of the great destructive scale of the storm, and the rising elevations and intact structures inland, which prevented the debris from being washed through as if on an inundated barrier island.

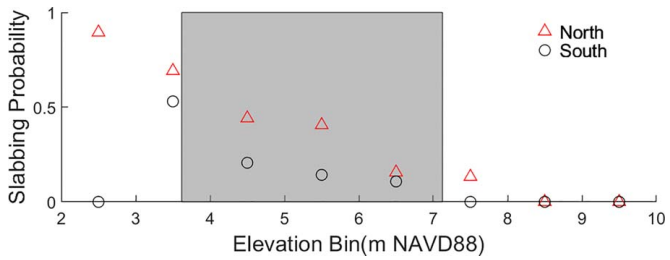

Fig. 13. (Color) Slabbing probabilities for all flood zones combined as a function of location. North Mexico Beach (triangle); South Mexico Beach (circle). The shaded region shows the range of observed high watermarks.

Many debris piles or clusters were large enough to be visible on aerial or satellite imagery. For this study, clusters are defined as a contiguous grouping of debris with a characteristic length scale of at least 5 m and are distinguishable on satellite images. Polygons enclosing clusters were generated manually using judgment, and are shown in Fig. 15. In total, 1,037 debris clusters were identified, with total plan areas of 28.0 ha (69.3 acres). Large clusters were often seen to be bounded on the landward side by either topographic high elevations (particularly for runup), intact vegetation (trees and bushes), and structures blocking further transport. These clusters tended to be composed of floating debris, while heavier masonry and concrete tended to stay near to their original locations.

In some cases, shown in Figs. 6(a) and 14(a) which depict elevations and imagery from the same region, debris clusters had very high heights above ground and may have been grounded during the storm, that is,, the cluster was higher than water levels and reached the ground, acting as a dam, collecting additional debris, and preventing further transport. Although, to the best of our knowledge, no systematic study has been carried out, very large clusters not backed by a surviving structure often had large debris objects (LDOs) such as transported houses, roofs, or other large objects as nuclei. Fig. 16 shows LDOs, defined here as transported intact or semi-intact structural assemblies or whole structures, travel trailers, and recreational vehicles (RVs). Although structures are clear when out of place, trailers and RVs are fundamentally mobile

Fig. 14. (Color) Examples of debris transport and deposition: (a) Western Mexico Beach (image courtesy of NOAA), showing large debris piles; (b) boats and terrestrial debris; (c) waverunner rental shack and other debris in forested area; (d) large pile of woody debris and transported A-frame house grounded next to larger building; and (e) 34 m-long section of Mexico Beach Pier deck grounded against houses. (Images (b–e) by authors.)

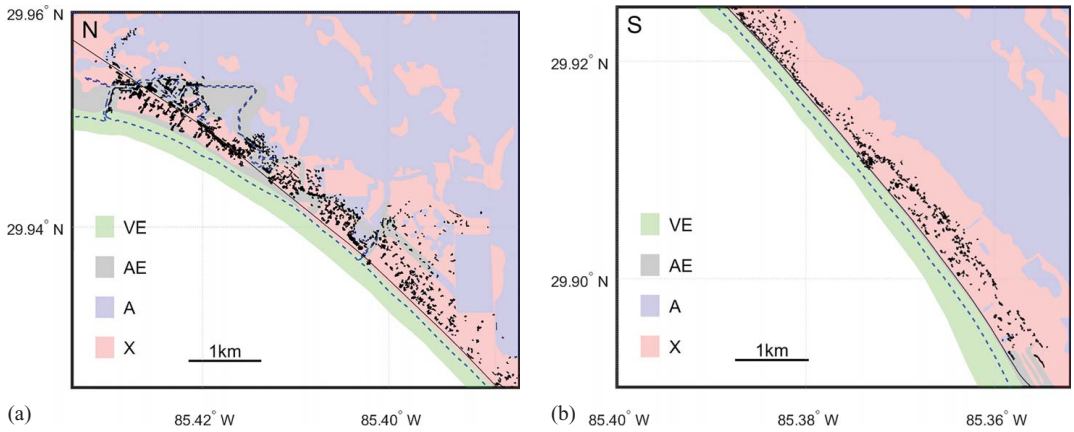

Fig. 15. (Color) Debris clusters in (a) North Mexico Beach area; and (b) South Mexico Beach area.

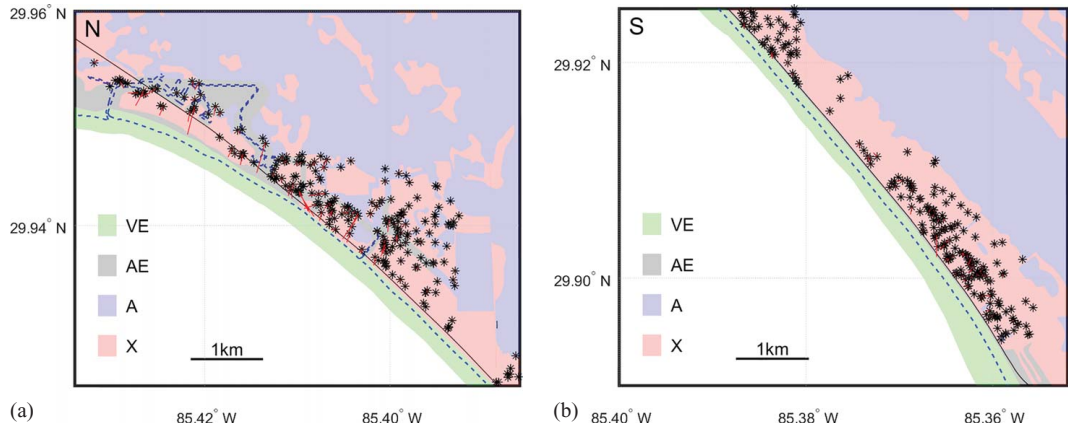

Fig. 16. (Color) Resting places for distinct LDOs identified in Mexico Beach post Michael: (a) North Mexico Beach; and (b) South Mexico Beach. Red lines indicate transport paths from original locations, where identified.

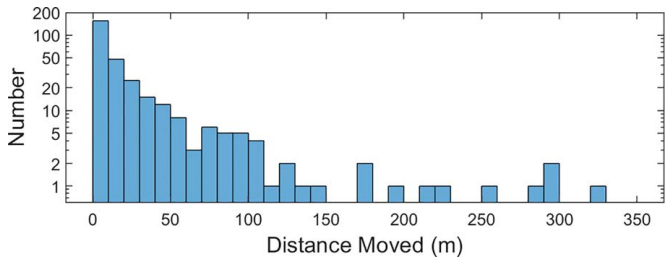

Fig. 17. (Color) Distance moved for LDOs in cases where original locations could be determined.

and could have been brought in poststorm but before the satellite photograph. These were only counted when tipped over, part of a larger debris cluster, tight against another structure, or in a strange position.

All LDOs originated somewhere and in many cases, it was possible to conclusively determine prestorm locations, in particular, for structures and structural assemblies. Fig. 17 shows distances moved by LDOs in the 301 cases where original locations could be identified. The large majority of LDOs moved relatively short distances, with 72% traveling < 25 m, 85% < 50 m, and 94% <100 m. The longest identified distance traveled by an LDO was 325 m for the roof of a house near the beach that was transported into an inland pine forest. Other studies have found that floating objects can travel large distances if unimpeded, with a largely intact house found to have floated 0.9 km from its piled foundations during Hurricane Ike (Kennedy et al. 2011). Longer distances are very possible, but with increasing distance of travel there comes the increased difficulty of identification. In this study, pine forests were inland from almost all development, limiting the potential distance of LDO travel.

Discussion and Conclusions

Mexico Beach was an unfortunate testbed for the effects of waves and surge on a variety of construction types. Maximum water levels exceeded BFEs by several meters, and deep inundation was recorded well past the 100-year floodplain. Inundation elevations from wave runup were greatest on the side of a small hill by the beach, and surge inundation appeared to be largest in the northwestern Mexico Beach. Inundation decreased significantly in southeastern Mexico Beach because this was both further from the storm landfall and showed the beginnings of sheltering by the St. Joseph Peninsula. Inundation levels were much higher than dune crests, and no dunes survived the storm in the Mexico Beach area. However, severe inundation was local to Mexico Beach, and larger nearby cities like Panama City and Panama City Beach had much lower water levels and correspondingly lower coastal damage.

Damage for low-lying properties near the Mexico Beach coast was near total, irrespective of construction type or age. Even in the X zones that are out of the 100-year floodplain, inundation damage was severe, with entire blocks of houses destroyed to their foundations. Many structures in this region were old and at low elevation; many owners did not have flood insurance. Damage decreased significantly with increasing structural elevation, as was expected, and with increasing distance inland. Structures that were not destroyed by waves and surge, in general, had significant wind damage, with severe roof damage typical for older structures not built according to the most recent building codes. Interior damage for flooded structures was significant. All utilities were lost during the storm and were slow to recover, with the notable exception of the cellular service. The storm generated large amounts of debris transported by waves and surge and created very large debris piles that generally accumulated against the side of a building, against the vegetation, or on a hill slope. This was close to a worst-case scenario for the Mexico Beach area. However, good design and construction were rewarded. By far the most obvious example was the famous Sand Palace, which survived Michael with relatively minor damage.

Some aspects of design and planning deserve more attention. Chief among them is the use of the 100-year floodplain to define areas of high risk and low risk. In wind engineering, Category II buildings (the most common type) use a 700-year return period for structural design (McAllister et al. 2018), which is much more severe. Earthquake design return periods for collapse vary depending on what is considered, but may specify a 2,475 year return period or the more severe 1% chance or less of collapse in 50 years, equating to a 5,000-year collapse event (National Institute of Building Sciences 2017). Tsunami standards in ASCE7-16 specify a 2% probability of being exceeded in 50 years, or a 2,475-year event (ASCE 2016). Therefore, if a structure is to last 50 years, it has a 40% chance of experiencing at least 1 design flood event and only a 7% chance of the design wind event, a 2% probability of the design tsunami event, and the same probability or lower of a design earthquake event. For older constructions that do not meet the 100-year standard, as was found in much of Mexico Beach, the probabilities of failure are much greater. These are extremely bad probabilities for flood design and are at the heart of why there is so much repeated damage and losses during storm surge and wave events. Design past the 100-year standard, or even recognition that areas past the 100-year flood plain have a real and non-negligible chance of inundation, damage, and collapse, would represent a fundamental change in outlook for coastal structure design, and one that is sorely needed.

Aspects that increased survival and reduced damage probabilities from waves and surge were:

1. Structural elevation above the highest observed HWMs, and much above the 100-year BFE.
2. Distance inland far enough that wave heights decreased to less damaging levels.
3. Attention to details of construction and higher quality building components, including foundations, and building connections. Wind damage was also greatly decreased by high quality roof, window, and framing details, and by adherence to the newest Florida Building Codes.

To decrease the chance of a repeat of this scenario, standards far beyond the 100-year flood are necessary. Draft revisions for FEMA Digital Flood Elevation Rate Maps in Bay County, FL (http://portal.nwfwmdfloodmaps.com/esri-viewer/map.aspx?cty=MexicoBeach), show large areas leveled by Michael remaining in the X zone (no requirement for flood insurance and stated 0.2% annual chance of flood hazard), with many others in the 9 ft or 10 ft (2.7–3.0 m) AE zone. The highest VE zone elevation in developed areas is 14 ft (4.3 m), with 12 ft (3.7 m) VE zones much more common. No buildings built to minimum required standards in these zones have a realistic probability of surviving Michael's successor.

Data Availability Statement

Damage data that support the findings of this study may be available from the corresponding author upon reasonable request.

Acknowledgments

This work was performed with funding from the National Science Foundation (Grant Nos. 1661015, 1822307, and 1841667), the National Institute of Standards and Technology, financial support from the Florida Division of Emergency Management Project No. B0021 DEM-HL-00004, the Joint Airborne Lidar Bathymetry Technical Center of Expertise, and the Applied Technology Council. Their support is gratefully acknowledged.

References

ASCE. 2016. *Minimum design loads and associated criteria for buildings and other structures*. ASCE/SEI 7-16. Reston, VA: ASCE.

Beven, J. L., II, R. Berg, and A. Hagen. 2019. *Hurricane Michael*. Tropical Cyclone Rep. No. AL142018. Miami National Hurricane Center.

Byrne, M. J., Sr. 2019. *Monitoring storm tide from Hurricane Michael along the northwest coast of Florida, October 2018*. Open-File Rep. 2019-1059. Reston, VA: United States Geological Survey.

Dal Pino, J. A. 2019. "The story of a survivor." *Structure* 26 (3): 34–36.

Dean, R. G., and R. A. Dalrymple. 1991. *Water wave mechanics for engineers and scientists*. Singapore: World Scientific.

Hatzikyriakou, A., N. Lin, J. Gong, S. Y. Xian, X. Hu, and A. Kennedy. 2016. "Component-based vulnerability analysis for residential structures subjected to storm surge impact from Hurricane Sandy." *Nat. Hazard. Rev.* 17 (1): 05015005. https://doi.org/10.1061/(ASCE)NH.1527-6996.0000205.

Kennedy, A., S. Rogers, A. Sallenger, U. Gravois, B. Zachry, M. Dosa, and F. Zarama. 2011. "Building destruction from waves and surge on the bolivar peninsula during Hurricane Ike." *J. Waterway, Port, Coastal, Ocean Eng.* 137 (3): 132–141. https://doi.org/10.1061/(ASCE)WW.1943-5460.0000061.

Landsea, C. W., and J. L. Franklin. 2013. "Atlantic hurricane database uncertainty and presentation of a new database format." *Mon. Weather Rev.* 141 (10): 3576–3592. https://doi.org/10.1175/MWR-D-12-00254.1.

McAllister, T. P., N. Wang, and B. R. Ellingwood. 2018. "Risk-informed mean recurrence intervals for updated wind maps in ASCE 7-16." *J. Struct. Eng.* 144 (5): 06018001. https://doi.org/10.1061/(ASCE)ST.1943-541X.0002011.

National Institute of Building Sciences. 2017. *Project 17 invitational workshop on seismic hazard mapping, April 11, 2017, Burlingame, CA*. Washington, DC: National Institute of Building Sciences.

Robertson, I. N., H. R. Riggs, S. C. S. Yim, and Y. L. Young. 2007. "Lessons from Hurricane Katrina storm surge on bridges and buildings." *J. Waterway, Port, Coastal, Ocean Eng.* 133 (6): 463–483. https://doi.org/10.1061/(ASCE)0733-950X(2007)133:6(463).

Roueche, D., et al. 2018. *SteerHurricane Michael: Field assessment team 1 (Fat-1) early access reconnaissance report (EARR)*. NHERI DesignSafe Project ID: PRJ-2111. https://doi.org/10.17603/ds2-vmqv-rj36.

Sallenger, A. H., Jr. 2000. "Storm impact scale for Barrier Islands." *J. Coastal Res.* 16 (3): 890–895.

Tajima, Y., T. Yasuda, B. M. Pachero, E. C. Cruz, K. Kawasaki, H. Nobuoka, M. Miyamoto, Y. Asano, T. Arikawa, and N. M. Ortigas. 2014. "Initial report of JSCE-PIC joint survey on the storm surge

disaster caused by Typhoon Haiyan." *Coastal Eng. J.* 56 (1): 1450006. https://doi.org/10.1142/S0578563414500065.

Tomiczek, T., A. B. Kennedy, and S. P. Rogers. 2014. "Collapse limit state fragilities of wood-framed residences from storm surge and waves during Hurricane Ike." *J. Waterway, Port, Coastal, Ocean Eng.* 140 (1): 43–55. https://doi.org/10.1061/(ASCE)WW.1943-5460.0000212.

Tomiczek, T., A. Kennedy, Y. Zhang, M. Owensby, M. E. Hope, N. Lin, and A. Flory. 2017. "Hurricane damage classification methodology and fragility functions derived from Hurricane Sandy's effects in coastal New Jersey." *J. Waterway, Port, Coastal, Ocean Eng.* 143 (5): 04017027. https://doi.org/10.1061/(ASCE)WW.1943-5460.0000409.